

Disorder Effect on the Vortex Pinning by the Cooling Process Control in the Organic Superconductor κ -(BEDT-TTF)₂Cu[N(CN)₂]Br

N. Yoneyama, T. Sasaki, T. Nishizaki, and N. Kobayashi
Institute for Materials Research, Tohoku University, Sendai 980-8577, Japan
(December 2, 2024)

We report the hysteretic magnetization measurements on κ -(BEDT-TTF)₂Cu[N(CN)₂]Br below T_c to investigate the second peak effect under the control of the cooling process from room temperature. The second peak of the magnetization was clearly observed below about 8 K for all the cooling process, and the dimensional crossover field is suggested to be about 200 Oe in the vicinity of the temperature independent minimum point between the central and second peaks. Faster cooling apparently suppresses the second peak structure, resulting in the reduced vortex pinning force. We propose that the domain structure of the disordered terminal ethylene groups of the BEDT-TTF molecules works as a possible origin of the effective vortex pinning site, which can qualitatively explain the behavior of the observed second peak.

74.70.Kn, 74.60.Ge, 74.60.Ec

I. INTRODUCTION

The κ -phase BEDT-TTF based organic superconductors, where BEDT-TTF is bis(ethylenedithio)-tetrathiafulvalene, feature the layered structure and the two-dimensional electronic properties, originating the interesting mixed state from a view of the vortex matter physics in which the high- T_c oxide superconductors have been vigorously investigated.¹ Several characteristic features on the mixed states have been observed in the organic superconductors; a wide reversible magnetization regime,² the second magnetization peaks,^{3–7} and the first-order phase transition between the vortex solid and liquid states.^{8–11} On the other hand, the molecular structure of BEDT-TTF can generally give a positional disorder, of which the terminal ethylene groups are thermally excitable between two conformations, “eclipsed” and “staggered”. In the present target compound, κ -(BEDT-TTF)₂Cu[N(CN)₂]Br, one of the ethylene groups on the molecule at room temperature is known to be disordered and the other ordered,¹² where the eclipsed conformation is stable. The conformational disorder then will be frozen by quenching, and can slightly affect the electronic state. The resistivity below about 80 K actually depends on the cooling rate,¹³ and in addition the superconducting transition temperature T_c is also reduced for the faster cooling rate.¹⁴ Moreover the report on the heat capacity suggests a glass transition caused by freezing of the motion in the ethylene group around 100 K.¹⁵ Accordingly the control of the cooling process plays a key role to investigate the electronic state of the present compound. Here, there are several contradictory reports on the magnetization hysteresis below T_c , that is, one shows an evident second peak,^{3–5} while the other is absent from the peak effect.^{9,16} Although this inconsistency is unclear, taking into account the significant role of the cooling process, we anticipate that to test the magnetization measurements under the control of the cooling

process will be a clue to give information on the origin of the peak effect in the present compound.

In this paper, we present the hysteretic magnetization measurements below T_c to investigate the second peak effect by controlling the cooling process. We propose that the domain structure of the disordered terminal ethylene groups works as a possible origin of the effective vortex pinning site, which will give the qualitative explanation on the behavior of the observed second peak.

II. EXPERIMENTALS

Single crystals were synthesized by means of electrocrystallization. All the measurements of the magnetization were performed using a SQUID magnetometer (Quantum Design, MPMS-5) for an identical single crystal with the dimension of $1.8 \times 1.6 \times 0.3$ mm³. No grease was used to avoid deformation of the sample. The scan length of 2.0 cm was employed. The magnetic field was applied perpendicular to the conduction plane. The cooling process was controlled from room temperature to 15 K as follows; (1) 0.17 K/min with 30 h anneal at 70 K (slow-cooled), (2) 15 K/min (rapid-cooled), and (3) 100 K/min (quenched). After all the sequential measurements of the quenched sample, the data taken in the slow-cooled process again were completely reproduced, suggesting no deterioration of the sample by quenching, such as micro cracks. We carried out the similar measurements for other two samples, which indicate the same results with the present report.

III. RESULTS AND DISCUSSION

Figure 1 shows the temperature dependence of the static magnetic susceptibility at 5 Oe. After subtracted the contribution of the core diamagnetization ($-4.8 \times$

10^{-4} emu/mol), the demagnetization factor was corrected using an ellipsoidal approximation. T_c 's defined as an intercept of the extrapolated lines of the normal and superconducting states are 11.9, 11.5, and 11.0 K in the slow-cooled, rapid-cooled, and quenched process, respectively. Lowering T_c in the faster cooling process is quantitatively consistent with the previous report.¹⁴ The magnetizations under a zero-field-cooled (ZFC) condition from above T_c (shielding curves) show almost the full Meissner volume. The negligible cooling-rate dependence of the ZFC magnetization demonstrates that the volume fraction is almost unchanged by the cooling process. On the contrary, the magnetization volumes under a field-cooled (FC) condition (Meissner curves) are relatively small, accompanied by a further suppression of the volumes with cooling faster (see the open symbols in Fig. 1). We note that the field of 5 Oe is not sufficiently smaller than $H_{c1}(0) = 19$ G,¹⁷ and thus the small FC magnetization volumes are explained by the incomplete exclusion of the magnetic flux. Moreover $H_{c1}(0)$ is likely to decrease with T_c in the fast cooling. Then the reduced field $H/H_{c1}(0)$ is increased, which can effectively enhance the incompleteness of the flux exclusion causing the further suppressed FC magnetization volumes.

Figure 2(a) shows the magnetic-field dependence of the magnetization at 5.5 K. The broad peak effect can be seen around 500 Oe below about 8 K for all the cooling process, as displayed in the magnetization hysteresis width ΔM (Fig. 2(b)–(d)). The peak height apparently decreases in the faster cooling as reported previously.⁵ In order to compare the cooling rate dependence of ΔM with different T_c 's, the critical current densities J_c are estimated at a reduced temperature t ($= T/T_c$). Figure 3 shows the magnetic-field dependence of J_c at $t = 0.41$, where the data of the quenched sample at 4.5 K are used, and the corresponding data at 4.7 K (rapid-cooled) and 4.9 K (slow-cooled) are calculated from a linear interpolation with the data at both 4.5 and 5.0 K, respectively. The estimation of J_c from ΔM was carried out through a standard Bean's model.¹⁸ Despite of considering the decrease of T_c , the critical current density clearly decreases in the faster cooling process, indicating the reduction of an effective vortex pinning. Cooling faster is known to induce the frozen disorder of the ethylene groups of the BEDT-TTF molecules, and then reduce T_c . Nevertheless, the effective pinning force in the present vortex system becomes weak with increasing the disorder. This result is not explained by the effect of the bulk pinning driven by the disorder. Here it should be noted that the size of the BEDT-TTF molecule (~ 3 Å) is much smaller than that of a vortex core ($2\xi_{\parallel}(0) \sim 50$ Å, where $\xi_{\parallel}(0)$ is the in-plane coherence length²). Thus, a disordered single molecule is too small to work as an origin of the vortex pinning site.

We next focus to the magnetic fields characterizing the peak effect as a function of temperature and cooling rate. Contrary to the peak effect of $\text{Bi}_2\text{Sr}_2\text{CaCu}_2\text{O}_8$,¹⁹

the structure of the peak in the present superconductor is quite broad and the magnetic field of the second peak cannot be defined without any ambiguity. We then introduce three trial fields distinctive of the peak position as follows; (1) the magnetic field of the minimum point between the central and second peaks (H_{\min}), (2) of the maximum point for the peak effect (H_p), and (3) of the inflection point (H^*) between H_{\min} and H_p estimated at the maximum in $d\Delta M/dH$ vs H curves (not shown in Figs). Each magnetic field is plotted in the T - H phase diagrams with overlaid for each cooling process, as shown in Fig. 4. Additionally plotted irreversibility fields (H_{irr} , open symbols) are defined using a criterion of $J_c = 2.0$ A/cm² (corresponding to $\Delta M = 1.0 \times 10^{-5}$ emu). As a function of temperature, H_p increases with reducing temperature for all the cooling process (Fig. 4(a)), while the temperature independence of H^* would be not significant because of the broad curvature of the $d\Delta M/dH$ vs H curves (Fig. 4(b)). The striking decrease of H^* and H_p by the fast cooling demonstrates that the broad peak is narrowed toward lower magnetic field regime as the cooling rate is fastened, namely, the appearance of the peak on the quenched sample is much more abrupt than those of the slower cooled condition. On the contrary, H_{\min} shows completely different behavior as displayed in Fig. 4(c), where the H_{\min} lines are piled around 200 Oe. Thus, H_{\min} is hardly changed by temperature and cooling process.

The peak effect of the present compound has been attributed to the dimensional crossover of the vortex system as a possible origin.^{3–5} A vortex line changes to two-dimensional (2D) pancake vortices with the decrease of the interlayer Josephson coupling in magnetic field above the crossover field $B_{\text{cr}} \approx \phi_0/(\gamma d)^2$, where ϕ_0 is the magnetic flux quantum, γ the anisotropy factor, and d the interlayer distance. Adopting the value of $\gamma = 180$ (Ref. 20) and $d = 15$ Å, one obtains $B_{\text{cr}} \approx 280$ G. The cooling rate independence of γ has not been known in the present compound as far as we investigated. However, even in the deuterated BEDT-TTF based-salt, which gives dramatically change in the electronic properties by cooling process control,²¹ the same values of γ with the present (non-deuterated) compound have been reported.²² Accordingly it is likely that the cooling process does not vary the anisotropy factor in this case at all. Hence we propose that the most appropriate magnetic field related to the dimensional crossover is supposed to be in the vicinity of $H_{\min} \sim 200$ Oe.

Before considering the pinning origin, we briefly mention the vortex bundle pinning around H_p . On the basis of the 2D collective pinning theory,^{1,23} the vortex bundle is formed above the magnetic field $H_1 \approx \phi_0^2 d J_c / \xi \epsilon_0 \sim 3$ kOe and above the temperature $U_p \approx d \phi_0 \xi J_c / c \sim 6$ mK, using an experimental value of $J_c \sim 10^3$ A/cm², where an energy scale $\epsilon_0 = (\phi_0/4\pi\lambda_{\parallel}(0))^2$ and $\lambda_{\parallel}(0) = 6500$ Å.¹⁷ Thus, a collective pinning of pancake vortices will be done around H_p since the present temperature regime

is quite larger than U_p while $H_p \ll H_1$.

Finally we discuss the puzzling origin of the vortex pinning resulting in the peak effect on the basis of the ordering of the ethylene group. First we focus the amount of the disordered molecules. Although the quenched condition must give the largest amount of disorders in the present case, the fraction of the disorders will be only about 5% as suggested by the ac calorimetry.¹⁵ We here insist on the existence of slight disorders even in the slow-cooled condition. The cooling rate dependence of T_c reported by Tokumoto¹⁴ can give information, where T_c monotonically decreases from 12.2 K to 11.7 K as the cooling rate increases from 10 K/min down to 0.02 K/min. T_c of 11.9 K at the rate ~ 0.2 K/min in this report shows a good agreement with our slow-cooled case, and thus T_c of the present sample can furthermore increase with much slower cooling. In other words, there will be some disorders even in the present slow-cooled condition, and the disordered molecules below a few % is controlled by the cooling process. Next we take into account the ordered domain structure. The existence of domain structures consisting of only staggered or eclipsed molecules are suggested by the study on the relaxation of the resistivity.²⁴ At high temperatures, the disorders will be the mixture of the staggered and eclipsed molecules and/or these micro domains. Then as the temperature is lowered, the stable conformation (eclipsed) gradually becomes dominant, and subsequently an ordered state will be formed by the growth of the eclipsed domains, where the remnant disorders, significantly dependent on the cooling process, weaken the superconducting state, causing the reduction of T_c by ~ 1 K. We here propose that the disordered domains work as a possible origin of the vortex pinning sites. Now it is fruitful to describe how a vortex is effectively pinned while the vortex pinning is collective in the magnetic field around H_p . Figure 5 schematically depicts such a situation on the domain structures at around 500 Oe (where the average vortex distance is about 2000 Å). The quenched process makes a frozen state at higher temperatures as a glassy state with an almost uniform distribution of the disordered molecules (Fig. 5(a)). In an ordered area whose size is smaller than the vortex core diameter, the vortices can easily hop on the basis of the valuable range hopping mechanism since the excitation energy is small. This situation is essentially similar with the amorphous superconductors,²⁵ and thus the small amount of the vortex pinning sites lead to the small peak of J_c . As the sample is moderately cooled (rapid-cooled condition), the ordered domain size will increase (Fig. 5(b)), by which simultaneously the disordered areas are partly divided. Finally in the slow-cooled condition, the wide ordered area with the remnant disordered domains will be formed (Fig. 5(c)), where the vortices will be pinned in the disordered domains. Here, one can expect that the main factor to determine the strength of the effective pinning force will be related to the average distance between the disordered domains. Thus the slow-cooled state displayed in

Fig. 5(c) gives much stronger effective pinning force than that in Fig. 5(b), leading to the enhancement of the peak effect.

IV. CONCLUSIONS

In conclusion, we reported the hysteretic magnetization measurements below T_c to investigate the second peak effect in the cooling rate of 0.17, 10, and ~ 100 K/min. The negligible cooling-rate dependence of the almost full volume in the superconducting state demonstrates that the volume fraction is unchanged by the cooling process. The second peak was clearly observed below about 8 K for all the cooling process, and the dimensional crossover field is supposed to be about 200 Oe in the vicinity of the minimum point between the central and second peaks. The second peak apparently decreases with cooling faster and thus the effective pinning force is reduced. We propose that the domains consisting of the disordered molecules works as a possible origin of the effective vortex pinning site, which can qualitatively explain the behavior of the observed second peak.

ACKNOWLEDGMENTS

This research was partially supported by the Ministry of Education, Science, Sports and Culture, Grant-in-Aid for Encouragement of Young Scientists, 12740374, 2000.

¹ G. Blatter, M. V. Feigel'man, V. B. Geshkenbein, A. I. Larkin, and V. M. Vinokur, Rev. Mod. Phys. **66**, 1125 (1994).

² M. Lang, F. Steglich, N. Toyota, and T. Sasaki, Phys. Rev. B **49**, 15227 (1994).

³ F. Zuo, S. Khizroev, G. C. Alexandakis, J. A. Schlueter, U. Geiser, and J. M. Williams, Phys. Rev. B **52**, R13126 (1995).

⁴ S. Khizroev, F. Zuo, G. C. Alexandakis, J. A. Schlueter, U. Geiser, and J. M. Williams, J. Appl. Phys. **79**, 6586 (1996).

⁵ H. Taniguchi and K. Kanoda, Synth. Met. **103**, 1967 (1999).

⁶ T. Nishizaki, T. Sasaki, T. Fukase, and N. Kobayashi, Phys. Rev. B **54**, R3760 (1996).

⁷ N. Yoneyama, T. Sasaki, N. Kobayashi, M. Inada, and S. Yamada, Synth. Met. **120**, 815 (2001).

⁸ T. Shibauchi, M. Sato, S. Ooi, and T. Tamegai, Phys. Rev. B **57**, R5622 (1998).

⁹ L. Fruchter, A. Aburto, and C. Pham-Phu, Phys. Rev. B **56**, R2936 (1997).

¹⁰ M. Inada, T. Sasaki, T. Nishizaki, N. Kobayashi, S. Yamada, and T. Fukase, *J. Low Temp. Phys.* **117**, 1423 (1999).

¹¹ M. M. Mola, S. Hill, J. S. Brooks, and J. S. Qualls, *Phys. Rev. Lett.* **86**, 2130 (2001).

¹² U. Geiser, A. J. Schultz, H. H. Wang, D. M. Watkins, D. L. Stupka, J. M. Williams, J. E. Schirber, D. L. Overmyer, D. Jung, J. J. Novoa, and M. -H. Whangbo, *Physica C* **174**, 475 (1991).

¹³ X. Su, F. Zuo, J. A. Schlueter, M. E. Kelly, and J. M. Williams, *Phys. Rev. B* **57**, R14056 (1998).

¹⁴ M. Tokumoto, N. Kinoshita, Y. Tanaka, T. Kinoshita, and H. Anzai, *Synth. Met.* **103**, 1971 (1999).

¹⁵ H. Akutsu, K. Saito, and M. Sorai, *Phys. Rev. B* **61**, 4346 (2000).

¹⁶ D. Prost, C. Lenoir, P. Batail, I. A. Campbell, and L. Fruchter, *Phys. Rev. B* **49**, 4023 (1994).

¹⁷ M. Lang, N. Toyota, T. Sasaki, and H. Sato, *Phys. Rev. B* **46**, 5822 (1992).

¹⁸ M. Tinkham, *Introduction to Superconductivity*, 2nd ed. (McGraw-Hill, New York, 1996), p. 178.

¹⁹ K. Kadokawa and T. Mochiku, *Physica C* **195**, 127 (1992).

²⁰ S. Kawamata, K. Okuda, T. Sasaki, and N. Toyota, *J. Low Temp. Phys.* **105**, 1721 (1996).

²¹ H. Taniguchi, A. Kawamoto, and K. Kanoda, *Phys. Rev. B* **59**, 8424 (1999).

²² H. Ito, M. Watanabe, Y. Nogami, T. Ishiguro, T. Komatsu, G. Saito, and N. Hosoi, *J. Phys. Soc. Jpn.* **60**, 3230 (1991).

²³ M. V. Feigel'man, V. B. Geshkenbein, and A. I. Larkin, *Physica C* **167**, 177 (1990).

²⁴ X. Su, F. Zuo, J. A. Schlueter, M. E. Kelly, and J. M. Williams, *Solid State Commun.* **107**, 731 (1998).

²⁵ S. Okuma and N. Kokubo, *Phys. Rev. B*, **61**, 671 (2000).

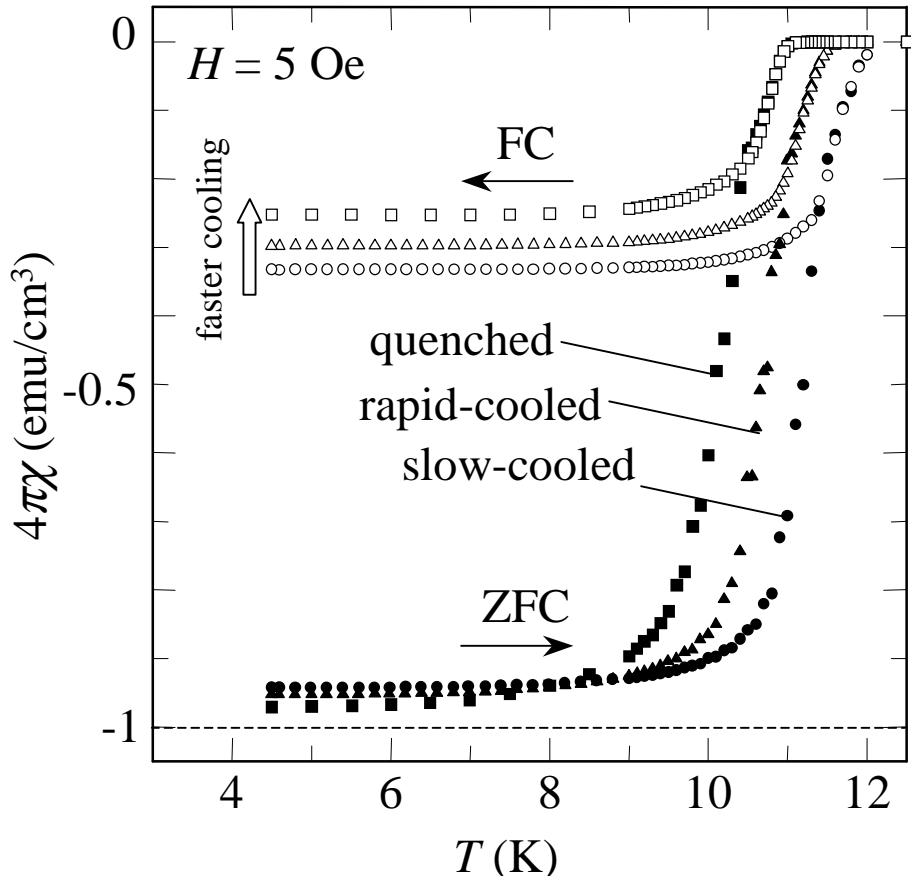


FIG. 1. Temperature dependence of the static magnetic susceptibility at 5 Oe. The closed and open symbols indicate the shielding curve measured under the zero-field-cooling condition (ZFC) and the Meissner curve under the field-cooling (FC), respectively, with overlaid for the slow-cooled (circles), rapid-cooled (triangles), and quenched (squares). The broken line shows the full-Meissner volume.

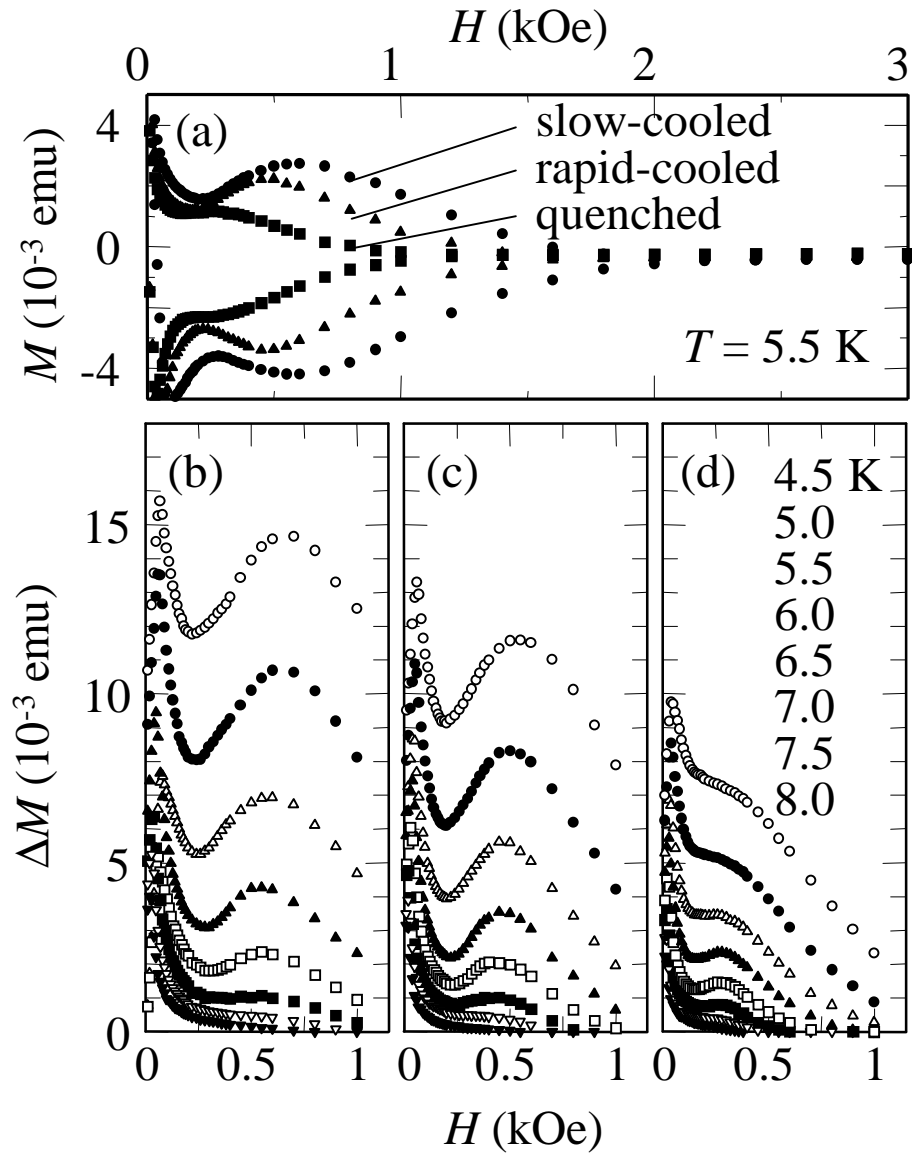


FIG. 2. Magnetic-field dependence of (a) the magnetization at 5.5 K, and the magnetization hysteresis width for cooling rates of (b) slow-cooled, (c) rapid-cooled, and (d) quenched condition, respectively, where the data at 4.5 to 8.0 K are overlaid.

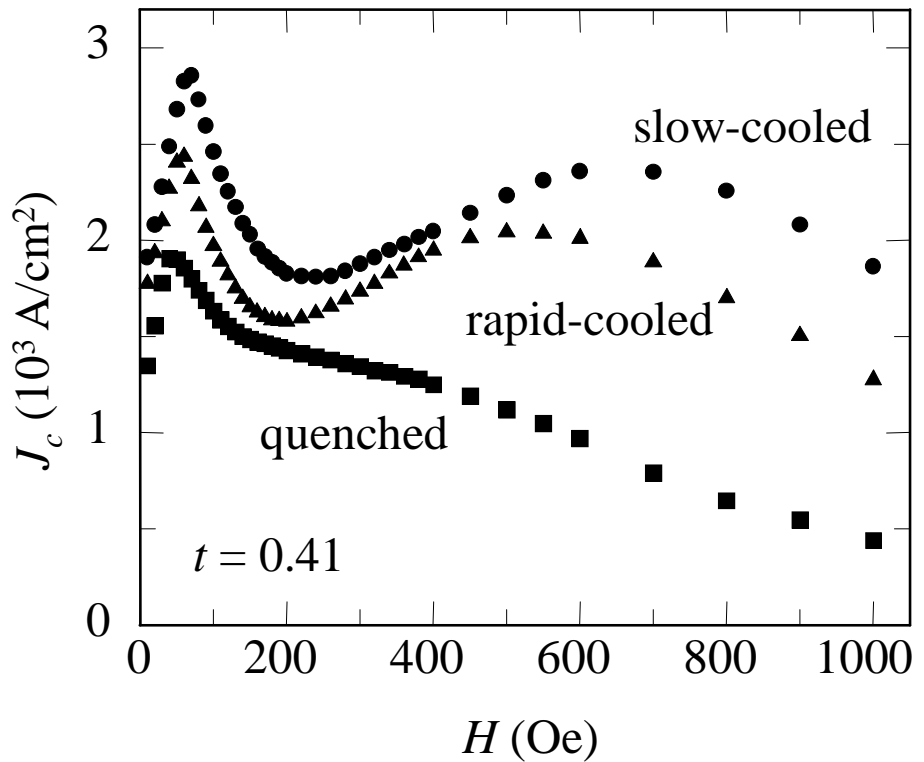


FIG. 3. Magnetic field dependence of the critical current densities at $t = 0.41$ estimated from $\Delta M(H)$ via a standard Bean's model.

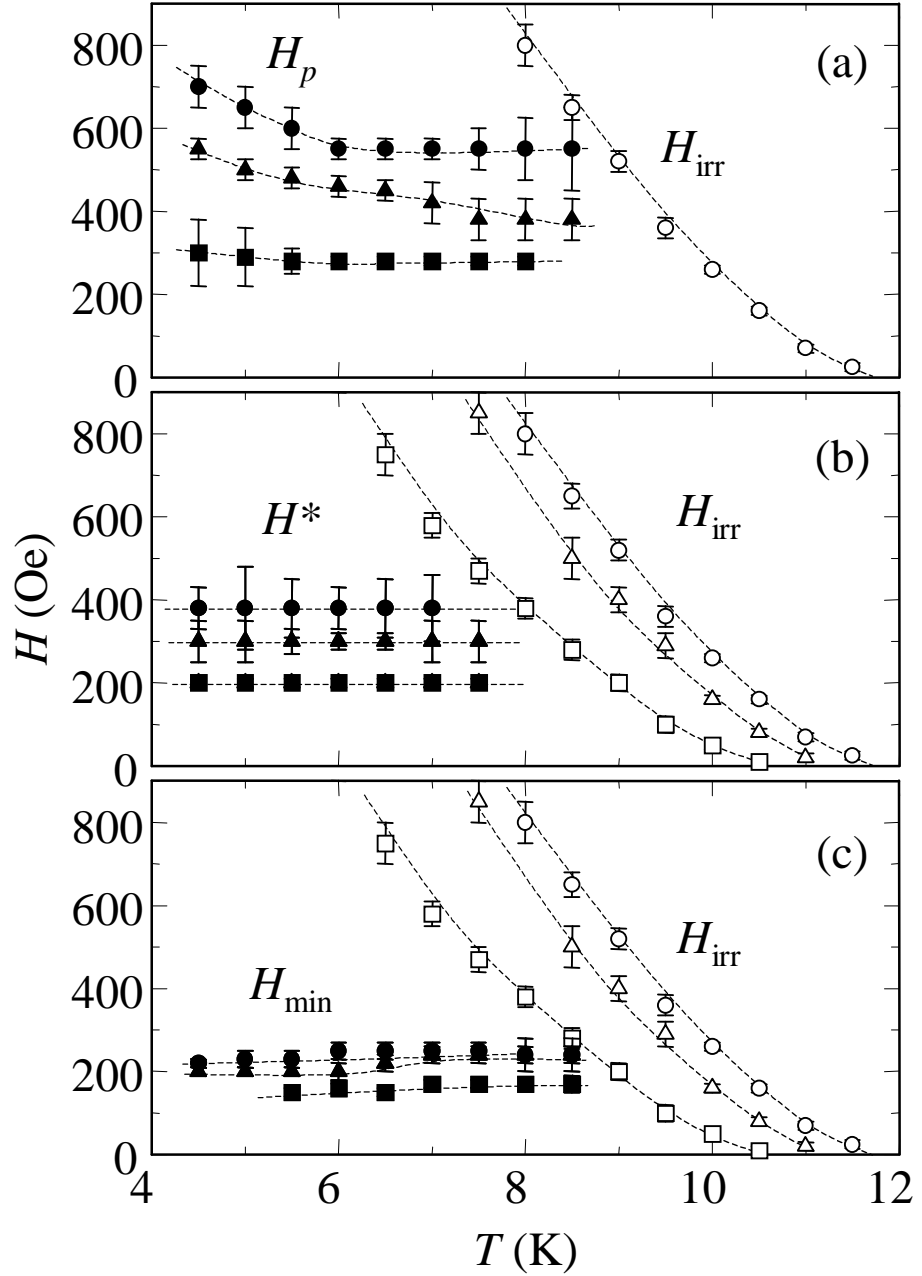


FIG. 4. Characteristic magnetic fields (closed symbols) as a function of temperature with overlaid for the slow-cooled (circles), rapid-cool (triangles), and quenched (squares): (a) H_{\min} , (b) H^* , and (c) H_p . H_{irr} (open symbols) are also plotted (partly omitted in Fig. 4(a) to simplify the Figs). The broken lines are guided for eyes.

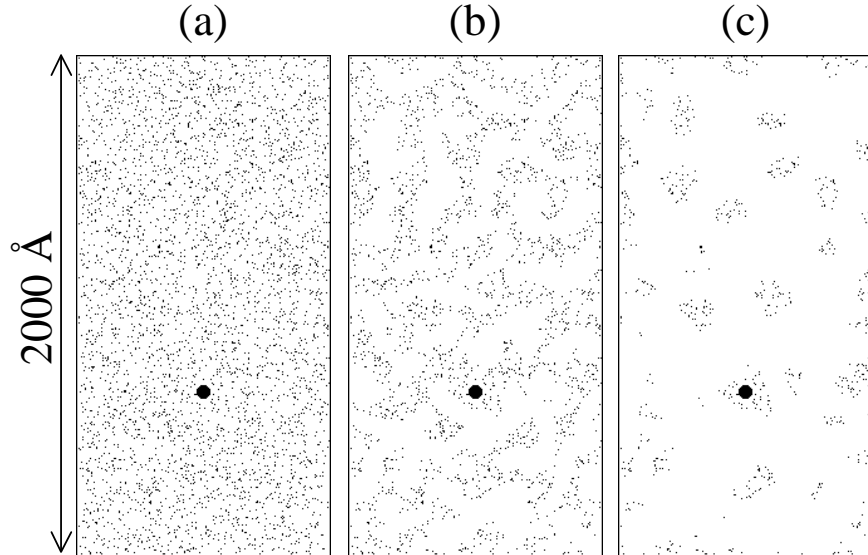


FIG. 5. Schematic view of the domain structure for (a) the quenched, (b) the rapid-cooled, and (c) the slow-cooled conditions, respectively, where 5% disorders are randomly distributed in the quenched condition. The scale of each map is about $1000 \times 2000 \text{ \AA}^2$, containing $\sim 8 \times 10^4$ BEDT-TTF molecules. The disorder molecules (dots; corresponding to about $5 \times 5 \text{ \AA}^2$) and a vortex normal core diameter (closed circle; 50 \AA) are described. Note that the ordered areas in (b) and (c) are made of (a) by hand.